We are IntechOpen, the world's leading publisher of Open Access books Built by scientists, for scientists

6,900
Open access books available

185,000
International authors and editors

200M
Downloads

Our authors are among the

154
Countries delivered to

TOP 1%
most cited scientists

12.2%
Contributors from top 500 universities



WEB OF SCIENCE™

Selection of our books indexed in the Book Citation Index in Web of Science™ Core Collection (BKCI)

Interested in publishing with us?
Contact book.department@intechopen.com

Numbers displayed above are based on latest data collected.
For more information visit www.intechopen.com



Chapter 18

Study of Multifunctional Nanocomposites Formed by Cobalt Ferrite Dispersed in a Silica Matrix Prepared by Sol-Gel Process

Nelcy Della Santina Mohallem, Juliana Batista Silva,
Gabriel L. Tacchi Nascimento and
Victor L. Guimarães

Additional information is available at the end of the chapter

http://dx.doi.org/10.5772/51154

1. Introduction

Surface science has a long history, involving the development of colloids, particulate material, thin films and porous materials. These materials have been known and used for centuries, without a profound knowledge of their real physical–chemistry characteristics. The detailed study of their properties was only possible with the emergence of more sophisticated spectroscopic techniques, and high-resolution eletron microscopes [1].

With the development of nanoscience and nanotechnology, new materials began to be studied like nanoparticles, porous materials that are formed by a network of nanoparticles, and nanocomposites. There are infinite possibilities of production of nanocomposites and one of them is the formation of nanoparticles inside porous matrices that can have their texture and morphology tailored by thermal treatment or templates [2].

For many applications, the textural properties, such as porosity and specific surface area, are as important as the chemical composition. Thus, the growing demand for porous products in the industry of nanotechnology, especially for magnetic nanocomposites, has led to the increase in the studies related to these properties [1, 2].

Magnetic materials have been used by man for centuries, since ancient people discovered the natural magnets called lodestones. The term "magnet" is used for magnetic materials that produce their own magnetic field. Other magnetic materials have magnetic proprieties only in response to an applied magnetic field. There are several types of magnetic materials

INTECH
open science | open minds

© 2012 Mohallem et al.; licensee InTech. This is an open access article distributed under the terms of the Creative Commons Attribution License (http://creativecommons.org/licenses/by/3.0), which permits unrestricted use, distribution, and reproduction in any medium, provided the original work is properly cited.

that have been used in diverse devices and systems for industrial products. Some traditional applications of these materials are in cores for motors, generators and transformers, microwave devices, magnetic media used in computers, recording devices, and magnetic cards, among others [3].

There are various metallic elements (Fe, Ni, etc) that have magnetic properties due to their crystalline atomic structure whose spins align spontaneously. Some alloys formed by metallic elements and others including the earth rare elements also have excellent magnetic properties (alnico, samarium-cobalt and neodymium-iron-boron magnets). Finally, the ferrites are a known class of magnetic materials formed by metallic oxides.

With the advancement of the material sciences and the emergence of the nanoscience and nanothecnology, new kinds of magnetic materials have been developed and studied in the last years, such as the magnetic nanoparticles, ferrofluids and magnetic nanocomposites. With these materials, new applications could be tested in areas such like electronic, catalysis and biomedicine, among others [4].

1.1. Ferrites

Ferrites are chemical compounds obtained as powder or ceramic body with ferrimagnetic properties formed by iron oxides as their main component, Fe_2O_3 and FeO, which can be partly changed by others transition metals oxide. The ferrites can be classified according their crystalline structure: hexagonal ($MeFe_{12}O_{19}$), garnet ($Me_3Fe_5O_{12}$) and spinel ($MeFe_2O_4$), where Me represents one or more bivalent transition metals (Mn, Fe, Co, Ni, Cu, and Zn). The ferrites are classified as "soft" or "hard" magnets, according to their magnetic properties, which refers to their low or high magnetic coercivity, respectively. Hard magnets are not easily demagnetized (curve a), due to their high coercivity and soft magnets are easily magnetized and demagnetized (curve b) with application of a magnetic field, due to their low coercivity. The characteristic magnetic hysteresis curves of these type of magnets are shown in Figure 1 [3,5,6].

The intermediate magnets, generally used in magnetic media, must have coercivity sufficiently high for withholding the information, but sufficiently low to allow for the information to be deleted (curve c) [5,6].

These magnetic ceramics [6] are important in the production of electronic components, since they reduce energy losses caused by induced currents and they act as electric insulators. They can be used in simple function devices such as small permanent magnets, until as sophisticated devices for the electro-electronic industry.

Recently, these materials have been discovered as good catalysts [7,8,9] and biomaterials [10,11].

http://dx.doi.org/10.5772/51154

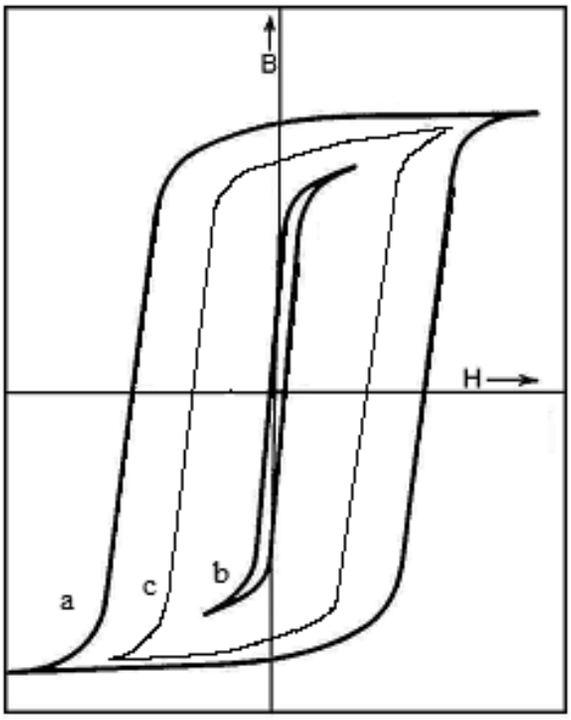


Figure 1. Magnetic hysteresis curves of (a) hard, (b) soft and (c) intermediate magnets.

1.1.1. Cobalt ferrites

Cobalt ferrite [3, 6], an intermediate magnet, is an important multifunctional magnetic material not only for its magnetic properties but also for its biomedical and catalytic applications, which depend on their textural and morphological characteristics. Cobalt ferrite, that has great physical and chemical stability, has been used in the production of permanent magnets, magnetic recording such as audio and videotape and high-density digital recording disks, magnetic fluids and catalysts. This ferrite has spinel inverse structure and exhibits a large coercivity, differently from the rest of the spinel ferrites. The magnetization of the $CoFe_2O_4$ crystal has anisotropic character because depends on its orientation. The strong magnetic flux promoted by the superexchange interaction is directioned along of the magnetization direction, and generally may be coinciding with the crystallographic axes. The magneto-crystalline anisotropy is related with the spin-orbit coupling. In polycrystalline materials, the magnetization measured corresponds to a mean value.

Recently these metal-oxide nanoparticles have been the subject of much interest because of their unusual optical, electronic and magnetic properties, which often differ from the bulk. These nanoparticles should have single domain, of pure phase, having high coercivity and intermediary magnetization [12].

The properties of the cobalt ferrite are changed according to the form of obtainment of the material, as bulk, particles or nanoparticles. The nanocrystalline particles have a high surface/volume ratio, and thus, they present different properties from those of bulk materials

Various authors [3,4,6,12,13] described the saturation magnetization and coercivity measured at room temperatures as a function of crystallite size and these values change from 30 to 80 emu g^{-1} for saturation magnetization and of 0.5 to 5.4 kOe for coercivity for crystallite size varying from 4 to 50 nm.

The effect of thermal vibrations is largest in very small particles, especially in materials with low anisotropy. The magnetic moments assume random orientations, at room temperature, for nanoparticles with size below the limit of 4-10 nm, resulting in superparamagnetic behavior [14-16].

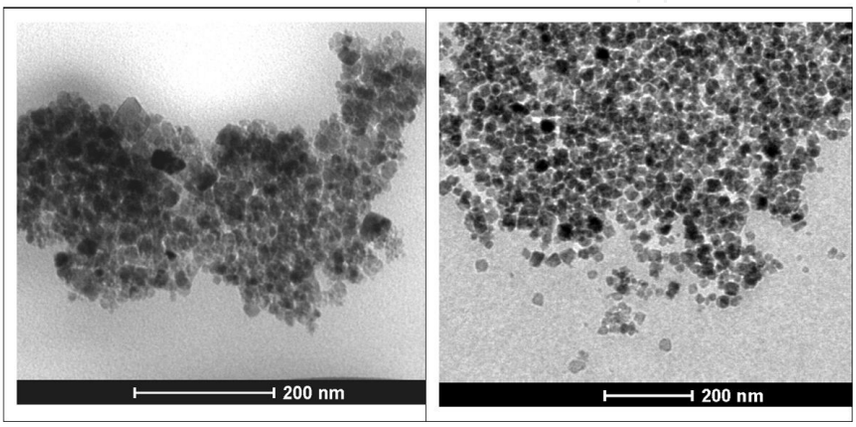


Figure 2. Cobalt ferrite nanoparticles obtained by (a) coprecipitation and (b) hydrothermal processes.

Superparamagnetic materials magnetize and demagnetize more easily than the other ones due to their dimension being equivalent to a magnetic domain. The magnetic domain of very small particles is different from that observed in bulk structures. There is a critical diameter below which the formation of a domain wall results in an increase of the total energy. The mono-domain size for $CoFe_2O_4$ nanoparticles has been estimated between 10 and 70 nm [17]. Crystallites with diameter smaller than 10 nm have superparamagnetic behavior, while with diameters larger than 70 nm (critical particle size/Dc) show multi-domain microstructure, with the consequent decrease in coercivity [17]. The existence of multiple domains separated by walls governs the magnetic behavior. The magnetization and demagnetization processes driven by an external field are characterized by the nonexistence of the hysteresis, characteristic of superparamagnetic materials.

Because of these interesting characteristics, nanocrystalline ferrites have been extensively studied with emphasis on the particle size variation and the influence of this variation in the mechanical, biomedical, magnetic and catalytic properties. In order to achieve desired properties, it is necessary to obtain high-density powders with a small and uniform grain size, and controlled stoichiometry. Hence, there is the need to develop fabrication processes relatively simple that induce the formation of controlled particle size materials. Some nanoparticles can be achieved more easily by using chemical methods [3,4,8,12,18,19], such as coprecipitation, hydrothermal synthesis and sol-gel process, among others, but generally the

http://dx.doi.org/10.5772/51154

nanoparticles tend to agglomerate due to their high reactivity. Figure 2 shows some cobalt ferrite nanoparticles obtained by coprecipitation and hydrothermal processes.

Due to these problems with high reactivity, agglomeration and aggregation of the nanoparticles, and the possibility of the development of new materials with peculiar properties, it has been synthesized nanocomposite materials formed by metal or metallic oxide nanoparticles dispersed in ceramic or vitreous matrices, avoiding the agglomeration and improving the dispersion and the distribution of the nanoparticles inside the system [20-34].

1.2. Nanocomposites

A composite is considered as a multiphase material with significant proportion of the properties of the constituent phases, whose final product has its property improved. There is the possibility of combining various types of materials in a single composite, in order to optimize their properties according to the desired application. When one of the phases has nanometric dimension, the system is called nanocomposite. [25,34].

Nanocomposite materials formed by metal or metallic oxide nanoparticles dispersed in ceramic or vitreous matrices have important applications due to the possibility of developing more reactive materials with new properties. The interest in the preparation of magnetic nanocomposites has increased in the last years due to the properties presented by these materials, which depends on the particle size, concentration and distribution of the particles in the matrix. Nanosystems such as Fe/SiO_2, Ni/SiO_2, Fe_3O_4/SiO_2, $CoFe_2O_4/SiO_2$, $NiFe_2O_4/SiO_2$ have been intensively studied in the last years, revealing different behavior from those of bulk magnetic systems and serving as models for the study of small particles [25-34].

The texture of the matrix and the interaction between the magnetic nanoparticles and the host matrix can be used to control the magnetic properties and the stability of these materials.

The magnetic nanoparticles dispersed in a inert matrix act as isolated nanomagnets, eliminating energetic losses, and producing the coupling between neighboring nanoparticles, which improve their magnetic properties. These nanocomposites can have high chemical and structural stability, high catalytic activity and high mechanical resistence.

The crystallite size control inside the matrix is justified by the existence of an average diameter range of single domain crystallites, between 10 nm < d < 80 nm, depending on the desired optimal magnetic properties [36,37]. When the ferrite concentration is low (< 30%), the crystallites are isolated, having single domains and showing superparamagnetism. Concentrations above 50% of ferrite provoke the agglomeration of the crystallites, which results in multi-domains [20]. Another important characteristic of nanocomposites in general is the texture of the matrix, as pore distribution, pore size and specific surface area, which has large influence in their final characteristics, as the transport and interaction of fluids within their connected network formed by micro, meso and macropores [38-41]. Important materials to be used as porous matrices are xerogels and aerogels, material obtained by sol-gel process.

In the last years, the sol-gel process has been used to produce magnetic nanocomposites by incorporation of ultra-fine magnetic nanoparticles with a high surface/volume ratio in different matrices. The nanocomposites formed have different properties from the magnetic bulk.

1.3. Sol-gel process

The sol-gel chemistry is based on mechanisms of hydrolysis and condensation of precursors containing metal (s) of interest, called "sol", resulting in an M-O-M oxide network that form a wet gel. There are two types of precursor: an aqueous solution of an inorganic salt or a metal alcoxide compound. The gel may be formed by polymerisation (gel polymer) or aggregation of colloidal particles subject to the physic-chemical conditions of the medium (colloidal gel). In either case, a three-dimensional solid network of the gel retains a liquid phase in its pores [42-49].

In practice, the network structure and the morphology of the final product depend on the relative contributions of the reactions of hydrolysis and condensation. These contributions may be controlled by varying the experimental conditions: the type of metal, type of organic binder, the molecular structure of the precursor, water/alkoxide ratio, type of catalyst and solvent, temperature and concentration of the alkoxide.

After the gelification, the wet gel is subjected to aging, to occur the polymerization processes, syneresis, and neck formation between the particles, leading to increase in connectivity and strength of the gel structure. The gel obtained is formed by a solid structure impregnated with the solvent. After the aging, various drying processes can be used to convert the wet gel in a porous material, denominated xerogel or aerogel.

The sol-gel process allows the preparation of materials in various forms such as powders, thin films, and monoliths, with desirable properties such as hardness, chemical durability, thermal and mechanical resistance and with different textures. The final product (xerogel or aerogel) can be tailored by different temperatures of thermal treatment leading to materials with different specific surface areas and porosities.

1.4. Xerogels and aerogels

The drying is one of the more important steps in sol-gel process because it is possible to obtain different materials by changing the drying routes. During the drying, the solvent adsorbed inside the porous gel is removed. During this process the gel network can collapse.

There are several types of drying processes; among them we can mention the controlled drying and the supercritical drying. In the controlled process, the solvent is evaporated slowly at room temperature and pressure, generating a contraction on the material, provoking the decreasing in the pore size due to the surface tension. The dry gels obtained by this process are called xerogels and have high porosity and specific surface area [27,50,51].

In the supercritical drying, the wet gels are put in a reactor at high temperature and pressure, above the critical point of the system, where there is no discontinuity between the liq-

http://dx.doi.org/10.5772/51154

uid and gaseous phase, avoiding capillary forces. The dry gels obtained are called aerogels and have higher porosity than the xerogel. [27,52,53].

In this work we studied the characteristics of nanocomposites formed by cobalt ferrites dispersed in silica matrix (xerogel and aerogel) obtained at different thermal treatment temperatures. Techniques such as X-ray diffraction (XDR), spectroscopy in the infra-red region, force atomic microscopy, transmission electron microscopy, scanning electronic microscopy equipped with energy dispersive X-ray (EDS) and wavelength dispersive (WDS) probes and gas adsorption were used to study the morphological and structural changes of the materials as a function of the thermal treatment temperature. The results were used to evaluate the mechanism of formation of the nanocomposites and relate their characteristics with magnetic and catalytic properties.

2. Experimental

2.1. Silica Matrix and Cobalt Ferrite Nanocomposite

The inert matrices formed by porous pure silica were obtained by mixing tetraethylorthosilicate, ethyl alcohol, water (1/3/10) and nitric acid, used as a catalyst. The nanocomposite precursor solution was obtained by mixing cobalt and iron nitrates, ($Co(NO_3)_2.6H_2O$ and $Fe(NO_3)_2.9H_2O$) with the matrix precursor, to form nanocomposites with 30 wt% of ferrite. The solutions were stirred for 1 h for homogenisation and left to rest for gelation, which takes place due to the hydrolysis and polycondensation of the metallic alkoxides. The wet gelswere aged at 60 °C for 24 h and dried at 110 °C for 12 h, leading to the formation of xerogels. Aerogels were formed by supercritical drying of the wet gels in an autoclave under 180 atm of N_2 and raising temperature up to 300 °C at 5 °C min^{-1}, temperature and pressure adequate to exceed the critical point of the mixture ethyl alcohol/water. The system was kept in this condition for 2 h. All xerogel and aerogel were heated between 300 and 1,100 °C for 2 h.

2.2. Caracterization Techniques

The structural evolution of the samples were analyzed in an X-ray diffractometer (Rigaku, Geigerflex 3034) with CuKa radiation, 40 kV and 30 mA, time constant of 0.5 s and crystal graphite monochromator. Crystallite sizes were determined by Scherrer equation (D = 0.9k/b cos h, where D is the crystallite diameter, k is the radiation wavelength and h the incidence angle). The value of b was determined from the experimental integral peak width using silicon as a standard. The values were corrected for instrumental broadening.

Spectra in the infrared region were obtained in an ABB Bomem equipment, model MB 102.

The composite compositions were evaluated by an electron microprobe (Jeol JXA, model 8900RL) with energy dispersive (EDS) and wavelength dispersive (WDS) spectrometers.

The morphology was obtained by scanning electron microscopy (high resolution SEM - Quanta 200 - FEG - FEI), by transmission electron microscopy (high resolution TEM - FEI) and by atomic force microscopy (Dimension 3000, Digital Instruments Nanoscope III - LNLS).

Sample textural characteristics were determined by N_2 gas adsorption (Quantachrome, model Nova 1200) at liquid nitrogen temperature. The samples dried at 110 °C were outgassed at 100 °C for 3 h. The others ones were outgassed at 200 °C for 3 h before each experiment. Specific surface areas and total pore volumes were obtained by the Brunauer-Emmett-Teller (BET) equation and the Barrett-Joyner-Halenda (BJH) method. These measurements were used to evaluate the total porosity, by the equation $P = 1 - \varrho_{ap}/\varrho_{th}$, where ϱ_{ap} is the apparent density and ϱ_{th} is the theoretical density. True densities were obtained in a helium picnometer (Quantachrome) and apparent densities were obtained by mercury picnometry.

The magnetic measurements were made in a Lake Shore vibrating sample magnetometry (VSM) at 300 K with a maximum applied magnetic field of 1 Tesla.

The nanocomposites were tested as catalysts in the oxidation of chlorobenzene in air. The catalytic reactions were carried out in a fixed bed reactor with 25 mg of catalyst. Chlorobenzene at 0.1% was introduced in the air stream (30 mL min-1) by a saturator at 0°C. The reaction products were analyzed by gas chromatography (Shimadzu/GC 17A) with a flame ionization detector (FID) and an Alltech Econo-Cap SE capillary column (30 mm 90. mm 9 0.25 lm).

3. Results and Discussion

The xerogels and aerogels silica matrices and nanocomposites were obtained in the monolithic form, without cracks.

3.1. Structural characterization

SiO_2 xerogel and aerogel treated up to 900°C exhibit amorphous behavior. A narrowing of the XRD peak accompanied by an increase in its intensity with increasing in the temperature of the preparation indicate an increase in the structural organization of the samples (Figure 3a and 3b). Characteristic reflections of crystobalite and tridimite appear at 1100°C for both the samples. The intensity of the xerogel peaks are larger than the aerogel ones.

The xerogel nanocomposites exhibit amorphous behavior up to 300 °C (according the X-ray difractometer resolution). $CoFe_2O_4$ crystalline particles with cubic spinel structure are detected by XRD inside the amorphous silica matrix above this temperature (Figure 4a). During the formation of the $CoFe_2O_4$ nanocrystals, no traces of intermediate products are found even at temperatures as high as 1100°C, indicating that the ferrite particles were formed without binding to the matrix. The magnetic nanoparticles also avoided the formation of either crystobalite or tridimite phases.

The aerogel nanocomposites exhibit amorphous behavior up to 700 °C (Figure 4b). The $CoFe_2O_4$ phase is detected by XRD only above this temperature.

http://dx.doi.org/10.5772/51154

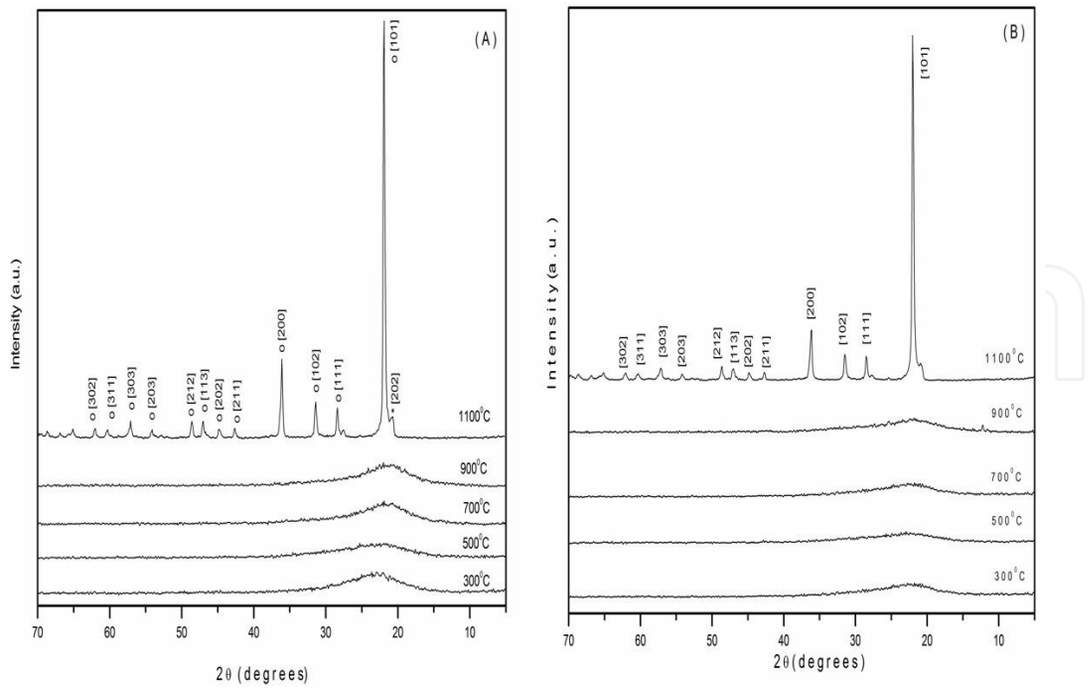


Figure 3. X-ray diffraction patterns of SiO_2 (a) xerogel and (b) aerogel, thermally treated in air for 2 hours at various temperatures. Crystobalite (o) and tridimite (*)

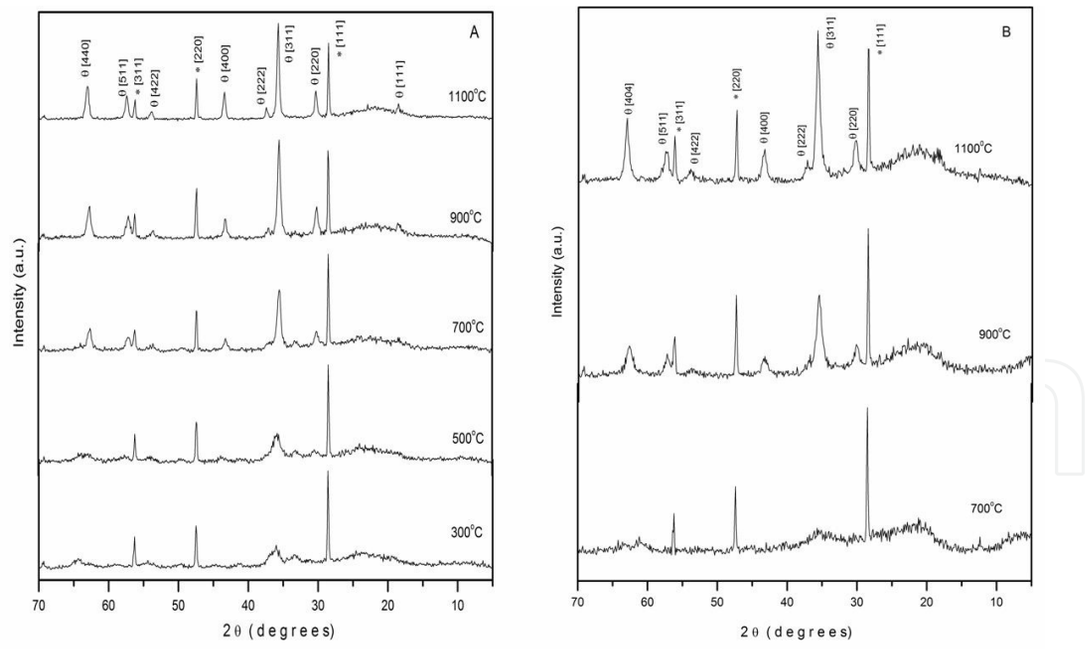


Figure 4. X-ray diffraction patterns of $CoFe_2O_4/SiO_2$ (a) xerogel and (b) aerogel, thermally treated in air for 2 hours at various temperatures. (Si) silicon, (Co) $CoFe_2O_4$.

Figure 5a shows the IR spectra of the xerogel samples obtained after heat-treating of the dried gel at various temperatures for 2 hours. The IR spectrum of the sample dried at 300°C has

absorptions characteristic of the silica network at 1080, 810, and 460 cm^{-1}. The 1086 cm^{-1} band with the shoulder at 1160 cm^{-1} is due to the asymmetric stretching bonds Si-O-Si of the SiO_4 tetrahedron associated with the motion of oxygen in the Si-O-Si anti-symmetrical stretching. The 810 cm^{-1} band is associated with the Si-O-Si symmetric stretch and the band at 461 cm^{-1} with either Si-O-Si or O-Si-O bending. The weak band in the 950cm^{-1} is due to stretching of the Si-OH. With increasing in temperature this band disappears due to the condensation reactions which change the Si-OH groups on Si-O-Si. The sample heated at 900^0C shows a decrease in intensity of the bands characteristic of the silica matrix, suggesting the rearrangement process of silica network, according XRD results. The aerogels have similar spectra.

Figure 5b shows the IR spectra of the xerogel nanocomposites. The IR spectrum of the sample dried at 300°C also has absorptions characteristic of the silica network and at 968 cm^{-1} we observed the band composed of the contributions from Si-O-H and Si-O-Fe vibrations. The band at 584 cm^{-1} is related to Fe-O stretching. The 968 cm^{-1} band disappears with the increase in temperature, showing that the weak bond between Si and Fe is broken [54]. We can observe a slight shift of the 584 cm^{-1} band to the left. Co-O stretching vibration characteristic band also appear at 461 cm^{-1}. The weak band at 675 cm^{-1} can be due to the cobalt ion in tetrahedral centers in the matrix pores.

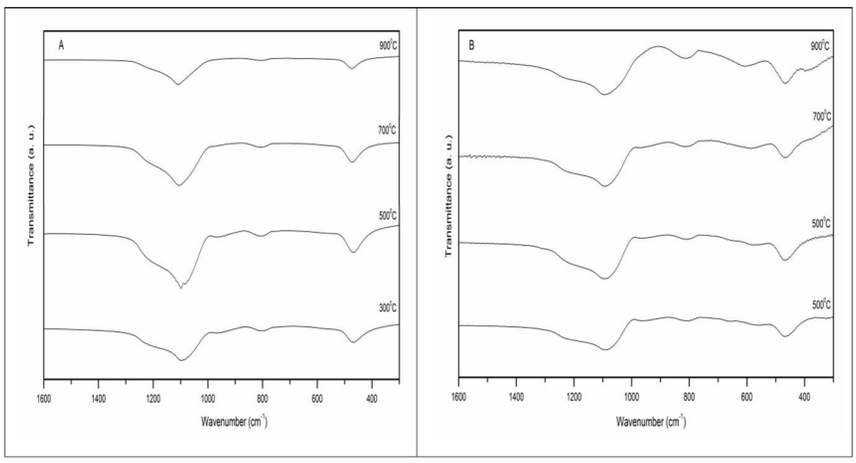


Figure 5. a) Infrared spectra of SiO_2 xerogel and (b) infrared spectra of $CoFe_2O_4/SiO_2$ xerogel treated at different temperatures.

IR spectra show that there was no formation of by-product, confirming X-ray diffraction results. All results suggest that the iron ions had interaction with the silica matrix when the nanocomposite was heated at low temperatures. These interactions disappeared with increasing in heating temperature, showing that they are weak bonds. These results suggest that the cobalt ions have been diffused by the porous matrix and have been bonded to iron to form the ferrite within the pores, without any binding or interaction with the silica network.

3.2. Textural Characteristics

3.2.1. Silica xerogels and nanocomposite xerogels

http://dx.doi.org/10.5772/51154

The xerogel is a typical porous material formed by a silica network with micro, meso and macro pores interconnected for all the bulk. Micro pores are pores smaller than 2 nm in diameter, meso pores are the pores with diameters between 2 and 20 nm, and macro pores are larger than 20 nm.

Monolithic porous matrices (Figure 6), without defects after drying, changed in size after thermal treatments at high temperatures. The shape of the samples were defined by the template. The silica xerogels are optically transparent in all temperatures of preparation.

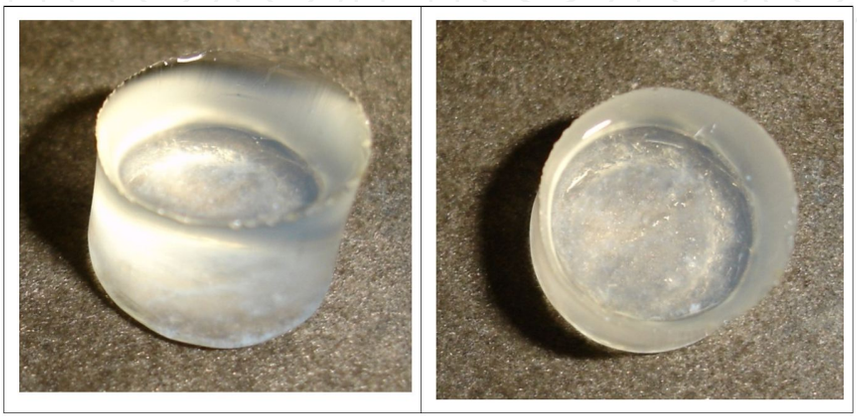


Figure 6. Silica xerogel.

AFM and TEM images (Figure 7) show the microstructure of a typical xerogel.

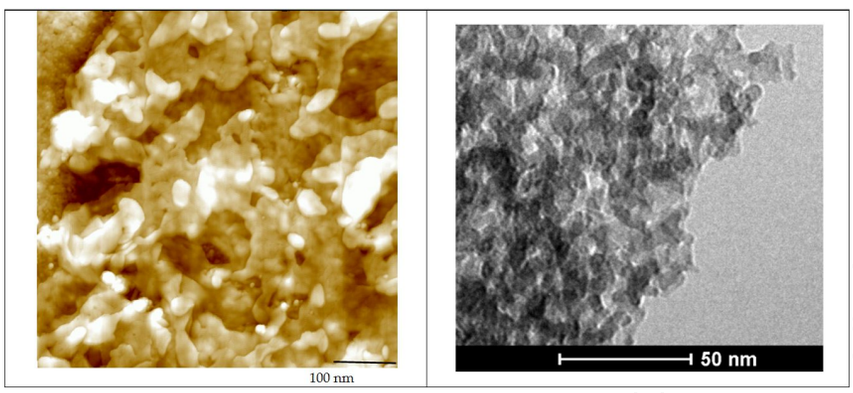


Figure 7. a) atomic force microscopy and (b) transmission electron microscopy images of a typical silica xerogel prepared at 500 °C.

The textural characteristics of the silica matrix xerogel changed substantially with thermal treatment. The specific surface area (Figure 8) decreased gradually for samples prepared above 300^0C, and between 500 and 700^0C decreased rapidly due to the densification process of the material. The silica xerogel porosity (Figure 9) remained constant for samples prepared up to 700 °C and decreased sharply until 900 °C, due to the collapse of the pores. The sample heated at 1100^0C became a material with a continuous silica network without pores.

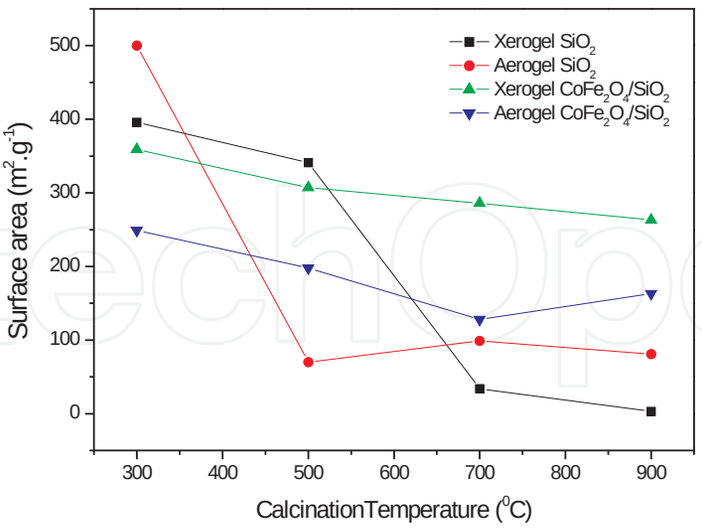


Figure 8. Variation of surface area as a function of temperature for composite $CoFe_2O_4$ in SiO_2 matrix and SiO_2. Error: 5%

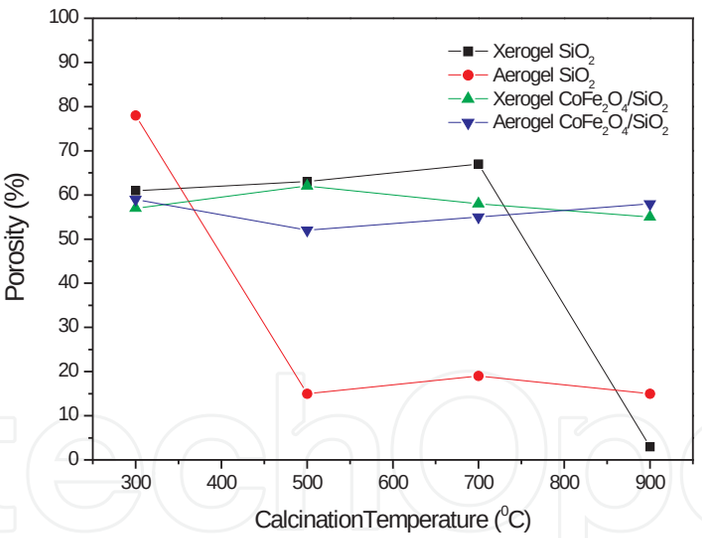


Figure 9. Variation of the porosity of silica matrices and cobalt ferrite nanocomposites as a function of temperature. Error: 5%

The formation of the ferrite nanoparticles inside the pores of the xerogel matrix reinforced the silica structure, keeping stable the pore network at high temperatures. In this case, the specific surface area decreases about 14% (Figure 8) and the total porosity remain almost constant between 300^0C and 900^0C (Figure 9). The shrinkage of the material structure occured only in samples heated above 900 ^{0}C.

http://dx.doi.org/10.5772/51154

Figure 10 shows the microstructure of the ferrite nanocomposite. With the increase in temperature, the ferrite grows inside the silica matrix.

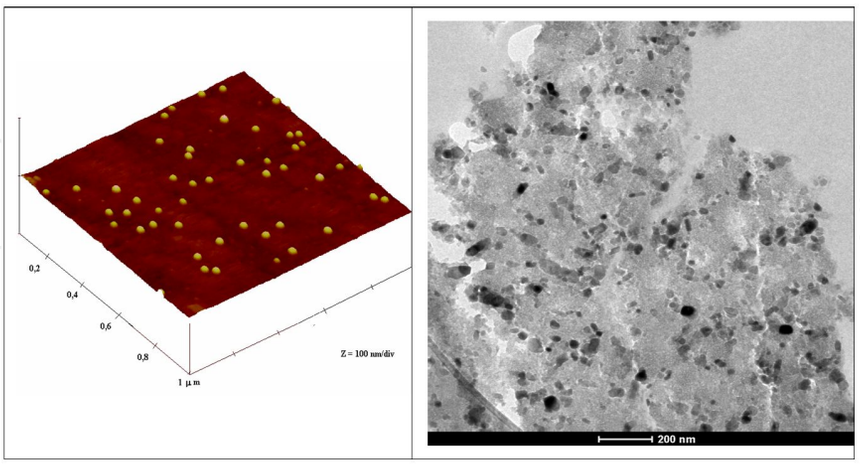


Figure 10. Atomic force microscopy and transmission electron microscopy images of cobalt ferrite nanocomposite prepared at 900 ^{0}C.

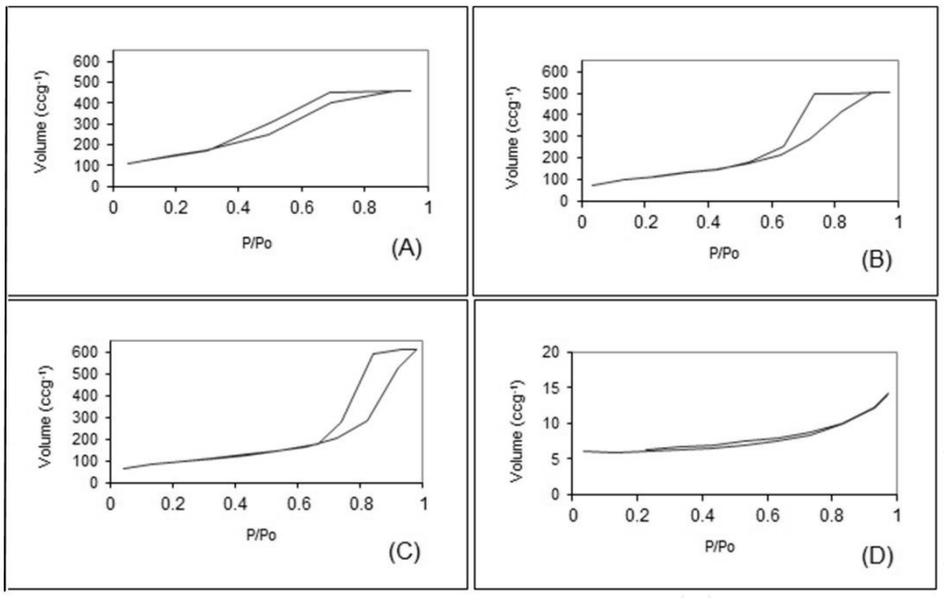


Figure 11. Adsorption-desorption isotherms of silica xerogels heated at (a) 300^{0}C, (b) 500^{0}C, (c) 700^{0}C and (d) 900^{0}C.

Figure 11 shows the adsorption-desorption isotherms of the SiO_2 xerogel at different thermal treatment temperatures. The sample prepared at 300^{0}C adsorbed about 450 $cm^3.g^{-1}$ of N_2. The xerogel adsoved more gas with increasing in the heating temperature due to the liberation of the organic compounds of their pores. The xerogel prepared at 700^{0}C adsorbed about 600 $cm^3.g^{-1}$. The isotherm of the sample heated at 300 ^{0}C presented characteristic intermediary of meso and microporous materials. The isotherms of the samples treated at 500^{0}C and

700^{0}C presented mesoporosity characteristics (isotherm type IV according the BDDT classification [39,41]). The samples heated at 900^{0}C presented isotherm type III, without hysterese, characteristic of non-porous material.

With the formation of ferrite nanoparticles inside the xerogel the material prepared at all temperatures became mesoporous corroborating the reinforcement in the xerogel microstructure.

All nanocomposite xerogel isotherms shown in Figure 12 are characteristic of mesoporous materials. The nanocomposite without thermal treatment adsorbed about 200 cm^3/g of N_2,

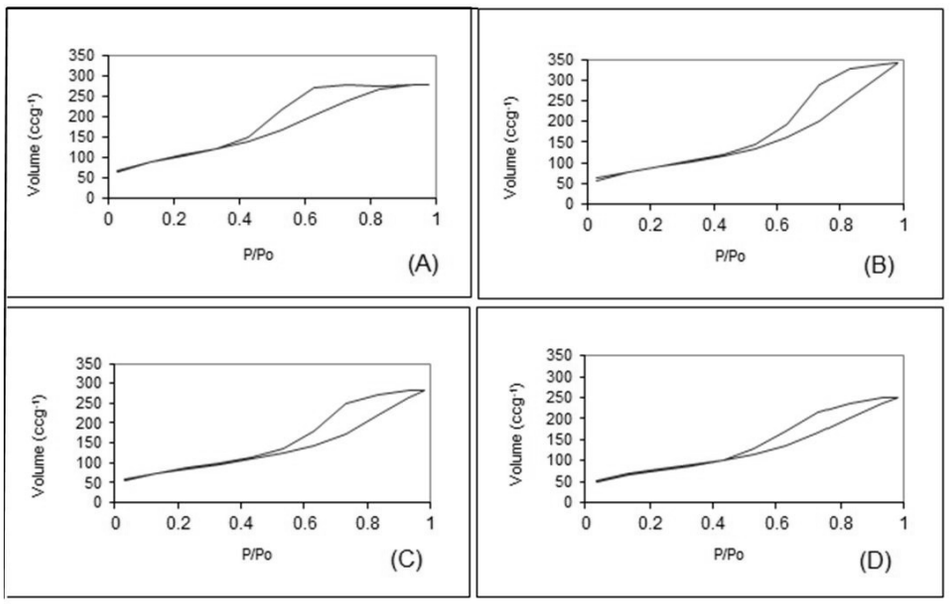


Figure 12. Adsorption/desorption isotherms of $CoFe_2O_4$ / SiO_2 xerogel, heated at (a) 300^{0}C, (b) 500^{0}C, (c) 700^{0}C and (d) 900^{0}C.

while nanocomposites prepared at higher temperatures adsorbed about 300 cm^3/g of N_2, due to the elimination of solvents. All isotherms (type IV [39,41]) presented characteristics of mesoporous materials. The hysteresis curves are type H2, characteristics of pores with indefinite form and size, according to the AFM and TEM images (Figure 10).

3.2.2. Silica aerogels and nanocomposite aerogels

The aerogel is an extremely porous material also formed by a silica network with micro, meso and macro pores interconnected for all the bulk. This material is much more porous than the xerogel, mainly as prepared. Monolithic aerogel matrices (Figure 13), without defects after drying, changed sharply in size after thermal treatments at high temperatures. The silica aerogels are slightly opaque due to the macroporosity, whose pores with the same size than the light wavelength interfere with the optical transparence.

http://dx.doi.org/10.5772/51154

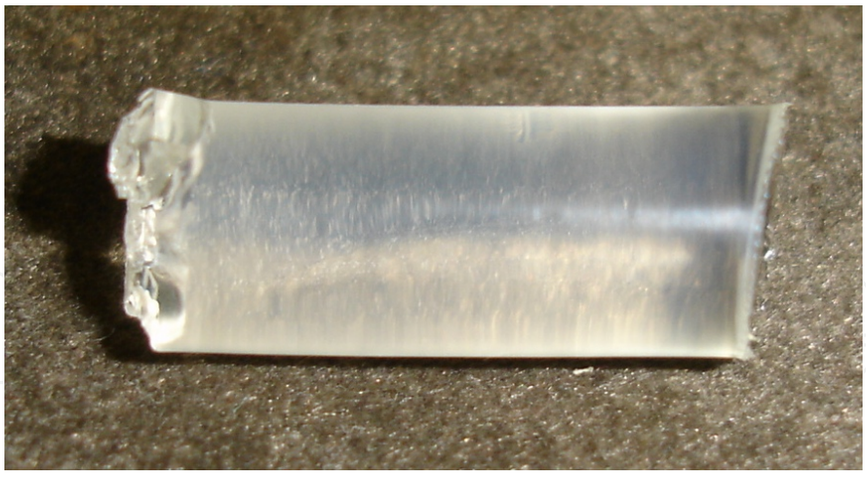


Figure 13. Silica aerogel.

Figure 14a shows a like-smoke structure of the aerogel. It is very difficult to obtain SEM and AFM images of this kind of material, due to their high porosity. Almost any preparation can destroy the network formed by the interconnection of the nanoparticles. Figure 14b shows the porous network structure of the aerogel, evidencing the necks formed by silica nanoparticles that led to the formation of micro, meso and macropores.

The as-prepared silica aerogels presented higher specific surface area and porosity than the xerogels obtained from the same precursor (Figure 8 and 9). Nevertheless, contrary to what happens with the xerogel, the porous network collapsed at low temperature of preparation

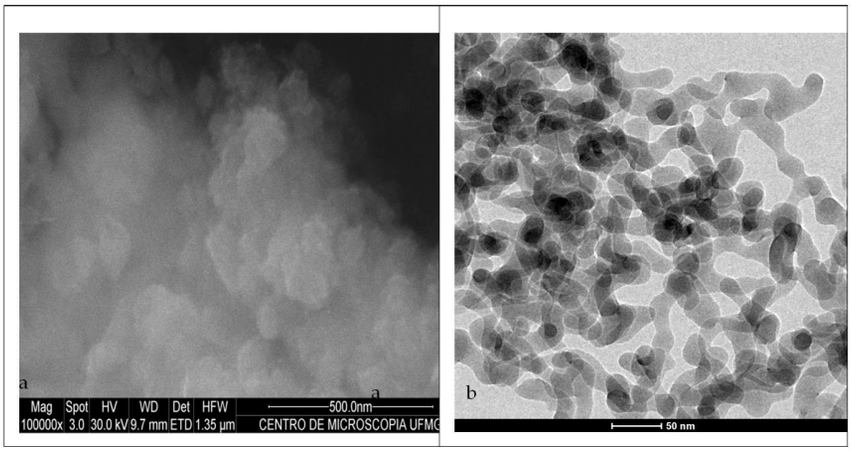


Figure 14. Scanning (a) and transmission (b) electron microscopies images.

of about 500 ^{0}C. The specific surface area and porosity changed from 500 m^2/g and 80 % for aerogels prepared at 300 ^{0}C to 50 m^2/g and 15 % for aerogels prepared at 500 ^{0}C. These values have been kept constant until temperatures of about 900 ^{0}C, when occurred the total collapse of the porous.The formation of the ferrite nanoparticles inside the pores of the aerogel matrix also reinforced their silica structure as happened with the xerogel matrices, but the

values of specific surface area were lower than the xerogel ones, as seen in Figure 8. In this case, the specific surface area Decreased of 250 to 150 m^2/g. The aerogel porosity values increased in comparison to the silica aerogel matrix and remained almost constant between 300^0C and 900^0C, with similar values to the xerogel ones. The shrinkage of the material network also occured above 900 ^0C.

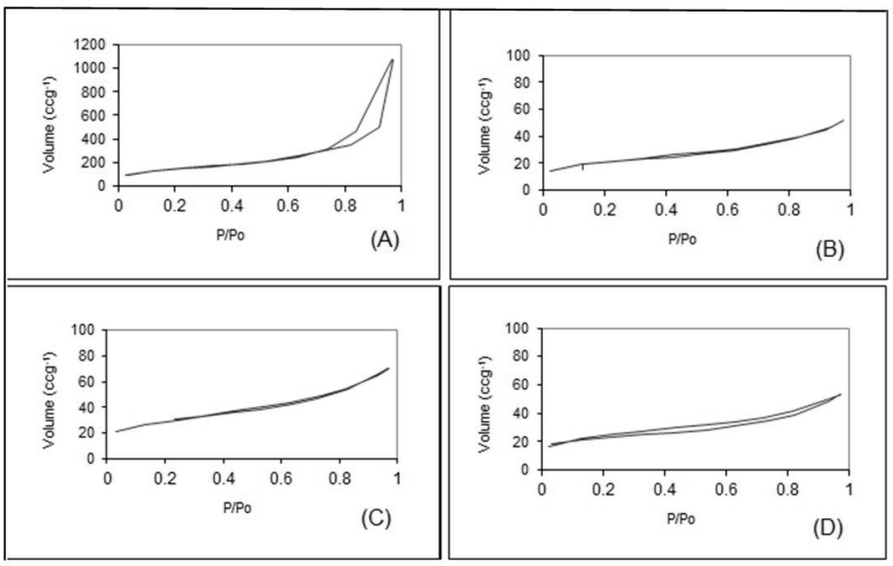


Figure 15. Adsorption-desorption isotherms of silica aerogels heated at (a) 300^0C, (b) 500^0C, (c) 700^0C and (d) 900^0C.

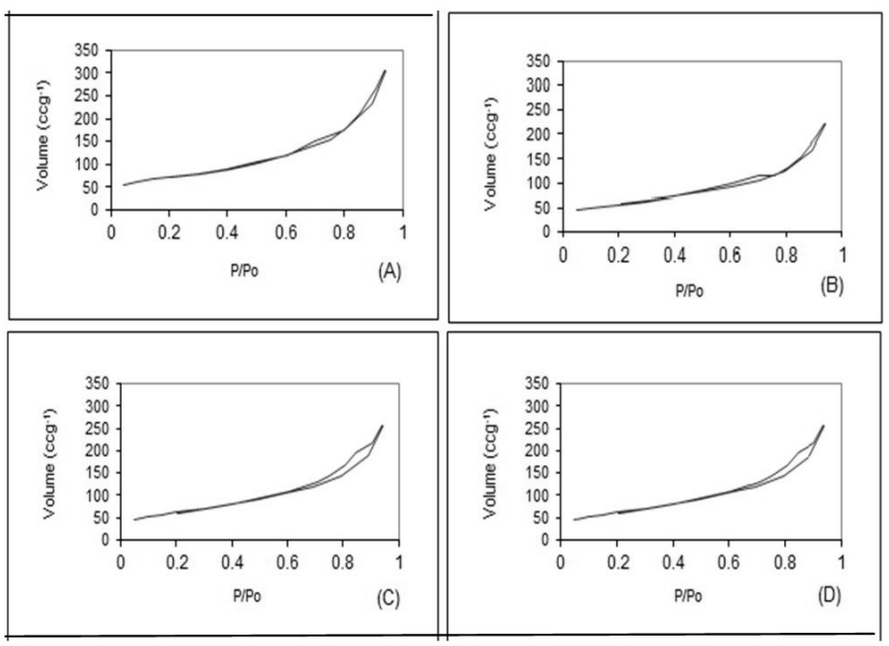


Figure 16. Adsorption/desorption isotherms of $CoFe_2O_4$ /SiO_2 aerogel obtained for sol-gel method and heated at (a) 300^0C, (b) 500^0C, (c) 700^0C and (d) 900^0C.

http://dx.doi.org/10.5772/51154

Figure 15 shows the silica aerogel isotherms. The isotherm of the sample prepared at 300^{0}C presented characteristics of mesoporous material (39,41), with large N_2 adsorption, of about 1200 $cm^3.g^{-1}$. This material is very fragile and when submitted at high heating temperatures its structure was annihilated, adsorbing only 60$cm^3.g^{-1}$ when prepared between 500 and 900 °C. Samples prepared between these temperatures did not present hysteresis and the adsorption-desorption curves are characteristics of macroporous materials [39,41].

All nanocomposite aerogel isotherms shown in Figure 16 are characteristic of macroporous materials. The as-prepared aerogel nanocomposite adsorbed ~300 $cm^3.g^{-1}$ of N_2, value much lower than that presented by the silica aerogel. The nanocomposites prepared at higher temperatures adsorbed about 250 $cm^3.g^{-1}$ of N_2, values larger than the silica aerogels prepared in similar temperatures.

3.2. Mechanism of formation

Backscattered electron images of the cobalt ferrite nanocomposites prepared between 300 and 700 °C showed defined white regions distributed throughout the sample, whose EDS analyses detected mostly the presence of cobalt clusters. In the gray region, Si, Fe, O and traces of Co were detected (Figure 17). The clusters disappeared with the increase in the preparation Temperature, suggesting that the cobalt ions diffused into the composite, binding to iron to form the ferrite. At temperatures above 900°C, EDS analyses detected a homogeneous distribution of Co and Fe in the composite. These results corroborate XRD and IR results.

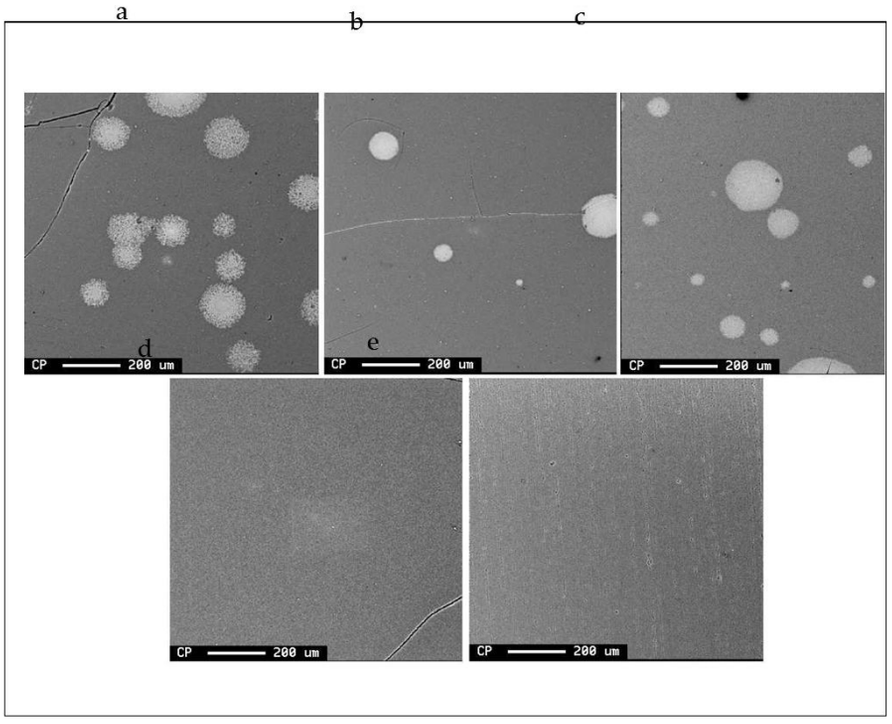


Figure 17. SEM images (backscattered electrons) of xerogels prepared at (a) 300^{0}C, (b) 500^{0}C, (c) 700 ^{0}C, (d) 900 ^{0}C and (e) 1100 ^{0}C.

Figure 18 shows the WDS mapping, used to confirm the mechanism of formation of nanoparticles inside the porous silica matrix. The different concentration of each metallic ion is shown by the color evolution. By this mapping, it is possible to observe with more acuity the diffusion process of the ions as a function of the temperature of preparation.

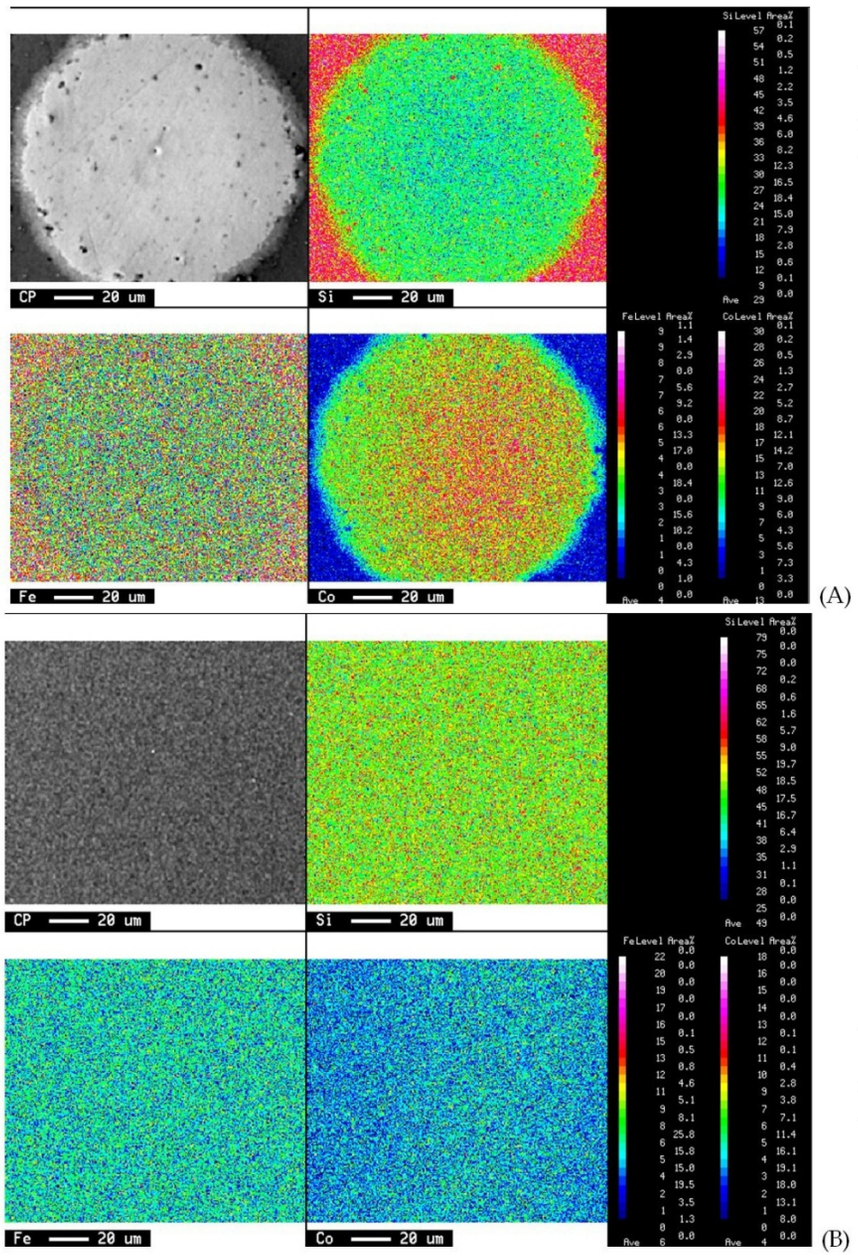


Figure 18. WDS mapping of the nanocomposite prepared at (a)500^{0}C and (b)1100^{0}C

Figure 19 shows the proposed model of the formation mechanism of the cobalt ferrite nanocomposites. The precursor solution is prepared by the mixing of Si alkoxide, alcohol, water and Fe and Co nitrates, and some catalysts (Figure 19 a). The wet gels are formed by hydrolysis and polycondensation of the sol constituents, maintaining the same ions distribution.

http://dx.doi.org/10.5772/51154

After drying, the elimination of water and organic residues occurs, and the xerogel (or aerogel) is formed by a silica network with iron ions distributed by the network and weakly bonded to the silicon (Figure 19 b). The Co ions are agglomerated in definite regions forming the clusters. With increasing temperature of preparation, the cobalt ions diffuse by the silica network, forming a chemical bond with the iron, which has its weak bond with the silicon broken (Figure 19 c). The pores diminish in amount and in size, and the magnetic nanoparticles grow inside these pores with the increase in temperature, leading to the encapsulation of the nanoparticles by the silica matrix (Figure d and e).

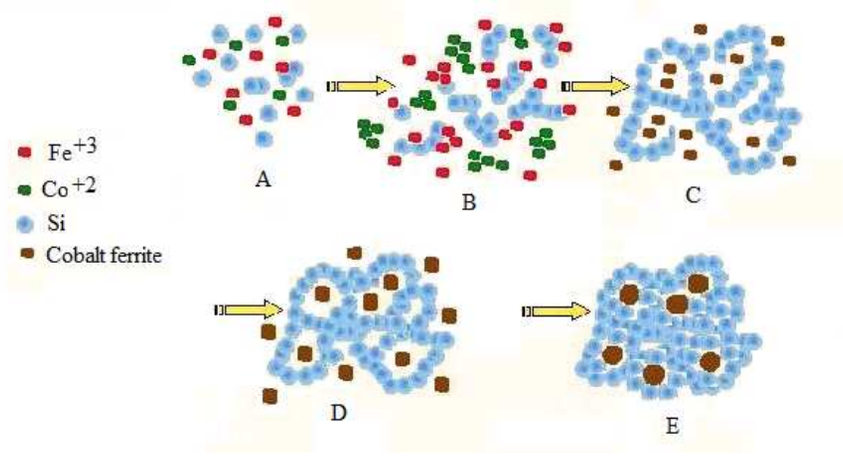


Figure 19. A proposed model of the formation mechanism of cobalt ferrite nanocomposites.

3.3. Properties and applications

Magnetic xerogels and aerogels can be considered as multifunctional materials due to the possibility of use their properties in multiple applications. The desired application can be obtained by tailoring the characteristics of the material.

Multifunctional materials are composites or systems capable of performing multiple functions simultaneously, depending of the involved phases, their structural, morphological and textural characteristics, improving system performances and reducing the redundancy between the composite components and their individual functions.

For example, porous xerogel and aerogel nanocomposites have interesting catalytic properties when tested in the oxidation of chlorobenzene in air. Figure 20 shows the performance of the xerogel nanocomposites prepared at various temperatures, compared to SiO_2. It is clear that the more porous nanocomposite had the best performance. Figure 21 shows the best performance of the xerogel and the aerogel prepared at 500 °C compared with ferrite powders obtained by coprecipitation.

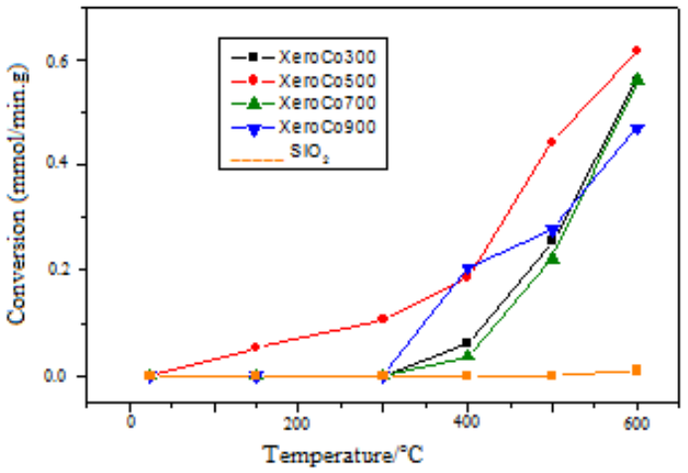


Figure 20. Catalytic oxidation of chlorobenzene in the presence of $CoFe_2O_4/SiO_2$ xerogels thermally treated at various temperatures.

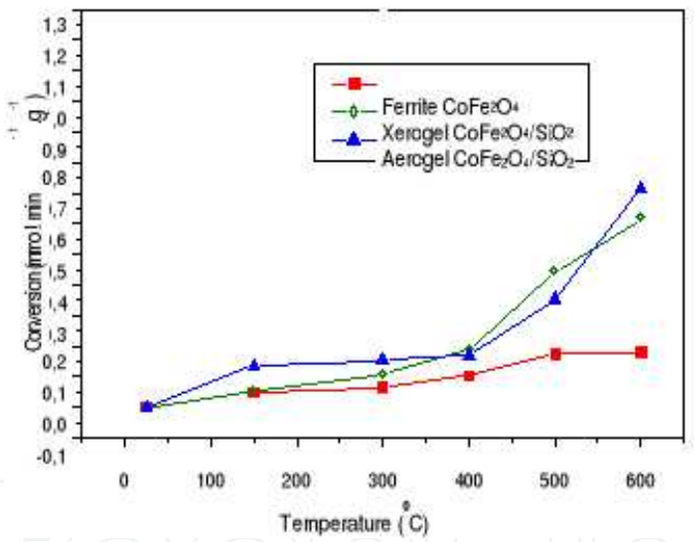


Figure 21. Catalytic oxidation of chlorobenzene in the presence of $CoFe_2O_4/SiO_2$ xerogels, aerogel and ferrite.

http://dx.doi.org/10.5772/51154

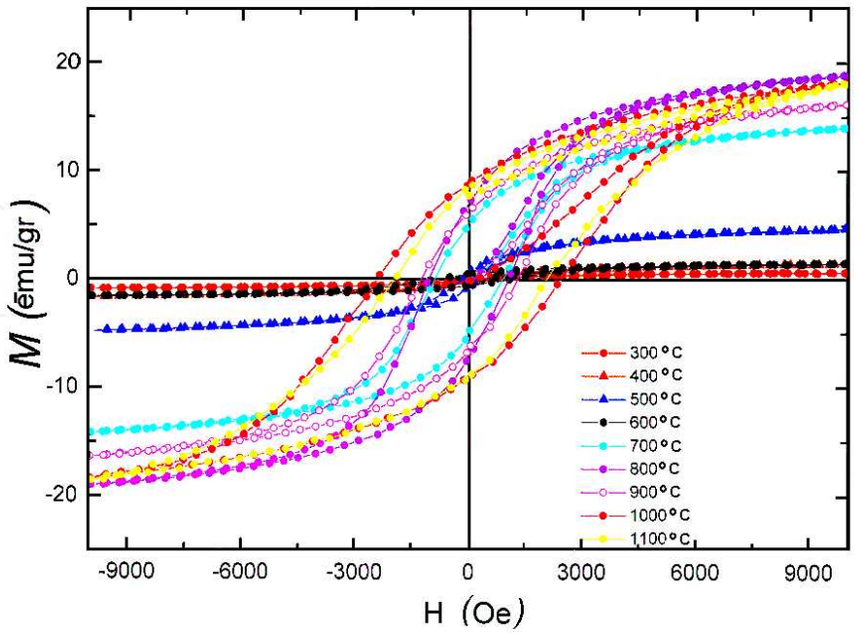


Figure 22. Hysteresis curves of the xerogel nanocomposites prepared at several temperatures.

The magnetic properties also are tailored by temperature. Figure 22 shows the hysteresis curve of the cobalt ferrite nanocomposites prepared at several temperatures, whos exerogels showed since superparamagnetic characteristics when prepared at low temperatures and intermediate magnetism at high temperatures. Due to these properties, these nanocomposites can be used as electronic devices or in biomedicine in cancer treatment by hyperthermia and drug release controlled by magnetic field.

4. Conclusion

Nanocomposites formed by cobalt ferrite nanoparticles dispersed in porous silica matrix ($CoFe_2O_4/SiO_2$) were prepared by the sol-gel process. The presence of the magnetic nanoparticles inside of the inert porous matrices of xerogels and aerogels reinforced their structure, avoiding large changes in specific surface area, porosity and in the microstructure of the matrix after preparation temperature, which varied between 300 and 900 °C. These characteristics influence the properties of the nanocomposites, such as their chemical reactivity, catalytic activity and magnetization. Due to the possibility of tailoring the textural and morphological characteristics of these types of multifunctional nanocomposites, they are promising candidates for many technological applications in electronic, catalysis and biomedical areas.

Acknowledgements

This work was supported by CNPq and Fapemig (Brazilian agencies). The authors acknowledge the use of the infrastructure of the Centre of Microscopy and Laboratory of Microanalyses/UFMG, and Laboratório Nacional de Luz Síncrotron – Brazil

Author details

Nelcy Della Santina Mohallem[1*], Juliana Batista Silva[2], Gabriel L. Tacchi Nascimento[3] and Victor L. Guimarães[1]

*Address all correspondence to: nelcy@ufmg.br

1 ICEx – Universidade Federal de Minas Gerais, Brazil

2 Centro de Desenvolvimento de Tecnologia Nuclear - CNEN/CDTN, Brazil

3 Nanum Nanotechnology Ltda, Brazil

References

[1] Moore, J. H., & Spencer, N. D. (2001). Ed. Encyclopedia of Chemical Physics and Physical Chemistry. Taylor & Francis

[2] Brushar, B. (2004). Handbook of Nanotechnology. New York, Springer.

[3] Valenzuela, R. (1994). Magnetic Ceramics. Cambridge, Cambridge University Press, 10.1017/CBO9780511600296.

[4] Coey, J. M. (2001). Magnetism in future. *Journal of Magnetism and Magnetic Materials.*, 226-230, 2107-2112.

[5] Snelling, E. C., & Giles, A. D. (1986). Ferrites for Inductors and Transformers. 2 a. ed. NY,

[6] Kingery, W. D., Bowen, H. K., & Uhlmann, D. R. (1976). Introduction to Ceramics 2. ed. New York, John Wiley & Sons.

[7] Rajaram, R. R., & Sermon, P. A. (1985). Adsorption and catalytic properties of $Co_xFe_{3-x}O_4$ spinels. *J. Chem. Soc., Faraday Trans.*, 81, 2577-2591.

[8] Ramankutty, C. G., & Sugunan, S. (2001). Surface properties and catalytic activity of ferrospinels of nickel, cobalt and copper, prepared by soft chemical methods. *Applied Catalysis A: General.*, 212, 39-51.

[9] Khalf-Alla, M., El -Salaam, A. B. D., Said, A. A., Hassan, E. A., & El -Wahab, abd. M. M. (1994). Structure and electronic effects of cobalt ferrites, CoxFe3-xo4 on catalytic decomposition of isopropyl alcohol. *Collect. Czech. Chem. Commun.*, 59, 1939-1949.

[10] Sharifi, H., & Shokrollahi, S. A. (2012). Ferrite-based magnetic nanofluids used in hyperthermia applications Ibrahim. *J. Magnet. Magnet. Mat.*, 324, 903-915.

[11] Bocanegra-Diaz, A., Mohallem, N. D. S., & Sinisterra, R. D. (2003). Preparation of a ferrofluid using cyclodextrin and magnetite. *J. Braz. Chem. Soc.*, 14, 936-941.

[12] Silva, J. B., Brito, W. ., & Mohallem, N. D. S. (2004). Influence of the heat treatment on cobalt ferrite nanocrystal powders. *Materials Science and Engineering. B, Solid State Materials for Advanced Technology*, 112, 182-187.

[13] Hench, L. L., & West, J. K. (1990). Principles of Electronic Ceramics. Wiley.

[14] Grigorova, M., Blythe, H. J., & Blaskov, V. (1998). Magnetic properties and Mössbauer spectra of nanosized $CoFe_2O_4$ powders. *J. Magnet. Magnet. Mat*, 183, 163-172.

[15] Qu, Y., et al. (2006). The effect of reaction temperature on the particle size, structure and magnetic properties of coprecipitated $CoFe_2O_4$ nanoparticles. *Mater. Lett*, 60, 3548-3552.

[16] Song, Q., & Zhang, Z. J. (2006). Correlation between spin-orbital coupling and the superparamagnetic properties in magnetite and cobalt ferrite spinel nanocrystals. *J. Phys. Chem. B. V. 110*, 23, 11205-11209.

[17] Chinnasamy, C. N., et al. (2003). Unusually high coercivity and critical single-domain size of nearly monodispersed $CoFe_2O_4$nanoparticles. *App. Phys. Lett.*, 83.

[18] Haneda, K., & Morrish, A. H. (1981). Magnetic structure of small NiFe2O4 particles. *J. Appl. Phys.*, 52.

[19] Haneda, K., & Morrish, A. H. (1988). Noncollinear magnetic structure of CoFe2O4 small particles. *J. Appl. Phys.*, 63.

[20] Silva, J. B. ., & Mohallem, N. D. S. (2001). Preparation of composites of ferrites dispersed in a silica matrix. *J.Magnet. Magnet. Mat*, 226, 1393-1396.

[21] Casula, M. F., Corrias, A., & Paschina, G. (2000). Nickel oxide-silica and nickel-silica aerogel and xerogel nanocomposite materials. *Journal Materials Reserch.*, 15, 2187-2194.

[22] Casula, M. F., Corrias, A., & Paschina, G. (2001). Iron oxide-silica aerogel and xerogel nanocomposite materials. *J Non- Crystall. Solids.*, 293-295, 25-31.

[23] Estounes, C., Lutz, T., & Happich, J. (1997). Nickel nanoparticles in silica gel: preparation and magnetic properties. *J. Magnet. Magnet. Mat.*, 173, 83-92.

[24] Huang, X. H., & Chen, Z. H. (2004). Sol-gel preparation and characterization of CoFe2O4-SiO_2 nanocomposites. *Solid State Commun.*, 132, 845-850.

[25] Kasemann, R., & Schmitd, H. K. (1994). A new type of a sol-gel derived inorganic-organic nanocomposite. *Materials Research Society.*, 346, 915-921.

[26] Silva, J. B. ., Diniz, C. F. ., Ardisson, J. D. ., Persiano, A., & Mohallem, N. D. S. (2004). Cobalt ferrite dispersed in a silica matrix prepared by sol-gel process. *Journal of Magnetism and Magnetic Materials*, 272-76, 1851-1853.

[27] Silva, J. B., Mohallem, N. D. S., Alburquerque, A. S., Ardisson, J. D. ., Novak, M. A., & Sinnecker, E. (2009). Magnetic studies of cofe2o4/sio2 aerogel and xerogel nanocomposites. *Journal of Nanoscience and Nanotechnology*, 9, 1-8.

[28] Souza, K. C. ., Mohallem, N. D. S. ., & Sousa, E. M. B. (2010). Mesoporous silica-magnetite nanocomposite: facile synthesis route for application in hyperthermia. *Journal of Sol-Gel Science and Technology*, 53, 418-427.

[29] Xianghui, H., & Zhenhua, C. (2006). Preparation and characterization of $CoFe_2O_4$/SiO_2 nanocomposites. *Chin. Sci. Bull.*, 51(20), 2529-2534.

[30] Xiao, S. H., Luob, K., & Zhanga, L. (2010). The structural and magnetic properties of cobalt ferrite nanoparticles formed in situ in silica matrix. *Materials Chemistry and Physics*, 123-385.

[31] Julian, C., Alcazar, G. A., & Montero, M. I. (1999). Mössbauer analysis od the phase distribution present in nanoparticulate Fe/SiO_2 samples. *Journal of Magnetism and Magnetic Materials.*, 203, 175-177.

[32] Rohilla, S., Kumar, S., Aghamkar, P., Sunder, S., & Agarwal, A. (2011). Investigations on structural and magnetic properties of cobalt ferrite/silica nanocomposites prepared by the coprecipitation method. *Journal of Magnetism and Magnetic Materials*, 323-897.

[33] Gharagozlou, M. (2010). Study on the influence of annealing temperature and ferrite content on the structural and magnetic properties of $x(NiFe_2O_4)/(100-x)SiO_2$ nanocomposites. *Journal of Alloys and Compounds*, 495-217.

[34] Gan, Y. X. (2012). Structural assessment of nanocomposites. *Micron*, 43-782.

[35] Sivakumar, N., Narayanasamy, A., Chinnasamy, C. N., & Jeyadevan, B. (2007). Electrical and magnetic properties of chemically derived nanocrystalline cobalt ferrite. *J. App. Phys.*, 102.

[36] Rajendran, M., Pullar, R. C., et al. (2001). Magnetic properties of nonocystaline $CoFe_2O_4$ powders prepared at room temperature: variation with crystallite size. *Journal of Magnetism and Magnetic Materials.*, 232, 71-83.

[37] George, M., et al. (2007). Finite size effects on the electrical properties of sol-gel synthesized $CoFe_2O_4$ powders: deviation from Maxwell-Wagner theory and evidence of surface polarization effects. *J. Phys. D: App. Phys.*, 40, 1593-1602.

[38] Meyer, K., & Lorenz, P. (1994). Porous solids and their characterization. *Cryst. Res. Technol.*, 29, 903-930.

[39] Lowell, S., & Shields, J. E. (1984). Power surface area and porosity. 2 a ed.,John Wiley N. Y.

[40] Gelb, L., & Gubbins, K. E. (1998). Characterization of porous glasses. *Langmuir*, 14, 2097-2111.

[41] Gregg, S. J., & Sing, K. S. W. (1982). Adsorption, surface area and porosity. 2 a ed. NY,

[42] Aegerter, M. A. (1989). Sol-Gel Science and Technology. .London World Scientific Publishing

[43] Brinker, C. J., & Scherer, G. W. (1990). Sol-gel science: The physics and chemistry of sol-gel processing. Academic Press Inc.

[44] Livage, J., Henry, M., & Sanchez, C. (1988). Sol-gel chemistry of transition metal oxides. *Prog. Solid State Chem.*, 18.

[45] Klein, E. . (1994). Sol-Gel Optics: processing and applications. Kluwer Academic Publishers.

[46] Mac, Kenzie. J. D. (2003). Sol-gel research- achievements since 1981 and prospects for the future. *J. Sol-Gel Sci. Techn.*, 23-27.

[47] Panjonk, G. M., Venkateswara, A., & Sawant, B. M. (1997). Dependence of monolithicity and physical properties of TMOS silica aerogels on gel aging and drying conditions. *Journal Non-Crystalline Solids.*, 209.

[48] Mohallem, N. D. S., Santos, D. I., & Aegerter, M. A. (1986). Fabricação de sílica vítrea pelo método sol-gel. Cerâmica, , 32(197), 109-116.

[49] Burneau, A., Gallas, J. P., & Lavalley, J. C. (1990). Comparative study of surface hidroxyl groups of fumed and precipitated silicas. *Langmuir*, 6, 1364-1372.

[50] Casu, M., & Casula, M. F. (2003). Textural characterization of high temperature silica xerogels. *Journal of Non-Crystalline Solids.*, 315, 97-106.

[51] Rao, A. V., Haranath, P. B. W., & Risbud, P. P. (1999). Influence of temperature on the physical properties of TEOS silica xerogels. *Ceramics International.*, 25, 505-509.

[52] Stolarski, M., & Pniak, M. S. B. (1999). Synthesis and characteristic of silica aerogels. *Applied Catalysis A: General.*, 177, 139-148.

[53] Schneider, M., & Baiker, A. (1995). Aerogels in catalysis. *Catal. Ver. Sci. Eng.*, 37, 515-556.

[54] Waldron, R. D. (1955). Infrared Spectra of Ferrites. *Physical Review.*, 99(6), 1725-1732.

IntechOpen

IntechOpen